2020 IEEE/RSJ International Conference on Intelligent Robots and Systems (IROS)
October 25-29, 2020, Las Vegas, NV, USA (Virtual)

Comparison between Stationary and Crawling Multi-Arm Robotics for In-Space Assembly

Katherine McBryan[1]

Abstract— **In-space assembly (ISA) is the next step to building larger and more permanent structures in orbit. The use of a robotic in-space assembler saves on costly and potentially risky EVAs. Determining the best robot for ISA is difficult as it will depend on the structure being assembled. A comparison between two categories of robots is presented: a stationary robot and robot which crawls along the truss. The estimated mass, energy, and time are presented for each system as it, in simulation, builds a desired truss system. There are trade-offs to every robot design and understanding those trade-offs is essential to building a system that is not only efficient but also cost-effective.**

I. Introduction

Scientists and engineers have been expounding the benefit of large space structures for years; whether talking about large solar panel arrays, large aperture telescopes, or large habitats [8], [3], [2], [7]. However, launch vehicle diameters are not increasing in size to meet these desires. For example, the James Webb Space Telescope (JWST)'s primary mirror has a final size of 6.5m while the launch vehicle has a diameter of 5m[18]. JWST, like many other space systems, deploys to reach its final size. However, as space structures become larger it is generally accepted that deployments will become too complex and the risk of failure too great[11], [6], [1], [4], [7].

In-space assembly (ISA) is a method of building large structures on orbit without relying on complex deployments or requiring a larger launch vehicle diameter. The International Space Station (ISS) was assembled on orbit by humans with help from robotic systems. Today, robotic ISA is a natural alternative to humans performing risky extravehicular activities (EVAs). Generally, the research into robotic systems for ISA falls into one of three categories: stationary or rigid mounted manipulators, free-flyers, and crawling/walking systems. This study focuses on stationary manipulators and crawling systems.

Stationary manipulators mount to the primary structure such as a satellite or space station and their base remains stationary relative to their workspace. The Japanese Remote Manipulators System (JEMRMS) is one such system. It is rigidly mounted on the ISS and is used to move pallets to the outdoor environment[10]. Power, communication and other functions are provided by the ISS.

Other examples of stationary manipulators include CIRAS and TALISMAN. CIRAS (Commercial Infrastructure for Robotic Assembly and Services) was a study done by Orbital ATK that uses two 15m TALISMAN (Tension Actuated Long Reach In-Space Manipulators), precision EBEAM welding, and a special jigging assembly robot to attach and detach a solar array[19]. Both these examples use very long manipulators ($>$ 10m) because the workspace of a stationary manipulator is limited by the length.

An alternative to the stationary manipulator design are free-flyers, small self-contained satellites with robotic manipulator(s). These systems have their own propulsion system which can greatly extend the workspace without increasing the length of the manipulators. However, free-flyers must carry their own power and are limited by propellant usage. ETS-VII was a free-flyer that studied robotic motion and assembly on orbit [9]. Suri et al. show that a free-flyer can be used, albeit with much development, for automated assembly in space [21].

Crawling systems are robots that adhere or grab onto the structure and move around. The individual 'legs' and 'feet' move from mounting point to mounting point or use end-effectors to grasp the structure. This offers some of the freedom and wider workspace of the free-flyer without being completely self-contained. The Space Station Remote Manipulator System (SSRMS) moves hand-over-hand (inchworm style) limited only by number of power-data-grappling-fixtures (PDGFs). Others, such as Carnegie Mellon University's Skyworker [20], do not require special grappling fixtures to walk along the structure. Lee et al. describe a 100m assembled telescope which can be assembled and maintained using a hexbot, a six-legged multi-arm system [12].

There have been many proposed robotic designs for ISA in each of these categories. New ISA designs are generally presented as single design points and do not offer comparison to other types of ISA systems. Although Nanjangud et al. [16] describes some of the trade-offs between different robotic assembly systems, this paper objectively compares a stationary and a crawling system as they construct a large space structure, a long truss made out of pre-constructed truss-segments. The goal of this paper is to study the trade-offs between a stationary and a crawling robot and how each design influences the payload structure and how the payload structure influences the robot designs. Section II presents an overview of the different robotic systems while Section III goes over the sizing for payload truss, the payload bay and the individual manipulators. Section IV briefly discusses the simulation and Section V presents the results for comparing the two robotic systems. Future work and conclusions can be found in sections VI and VII, respectively.

[1]Katherine McBryan is a researcher at the US Naval Research Laboratory, Washington DC 20375, USA katherine.mcbryan@nrl.navy.mil

II. Overview

In order to quantitatively compare the stationary and crawling robotic systems, they are designed to assemble the same planar space truss. Due to the planar nature of this study, all manipulators have two main links and 3 degrees-of-freedom (DOF). The last DOF, near the tool-tip, is to ensure the tool can attach to a payload at a pre-determined angle. For the dexterous arms, the desired tool-tip angle is determine by the structural design of the truss segments. Similarly, the angle for the positioning leg(s) is determined by the structural design of the payload bay.

The stationary robotic system is similar in design to many existing long-reach space manipulators with the exception of the payload bay. It consists of one positioning leg, a payload bay which holds all the truss segments, and two dexterous arms which handle the payload segments that are used to assemble the truss. The positioning leg is rigidly mounted to the primary structure and is used to move the payload bay and the two dexterous arms into position. Once in position, the two dexterous arms lower a truss segment from the payload bay into the final assembly. The dexterous arms then retract back to their starting location and the positioning leg moves the payload bay to the next location. Once the truss is assembled, the positioning leg returns to the initial position.

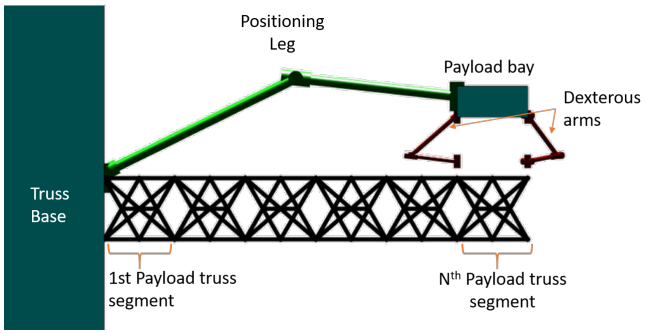

Fig. 1. Stationary Robot System

The crawling robotic system has two positioning legs, a payload bay, and two dexterous arms. The two positioning legs start at the same mounting point as the stationary system. After placing the first truss segment, the legs re-locate one at a time to the edge of the newly attached truss segment. After both legs have moved, they work together to re-position the payload bay readying them to place the next truss piece, see Figure 2. Once in position, the two dexterous arms lower the truss segment into place using the same motion as the stationary system. In this study, the arms and legs do not move at the same time. However, more complex motion planning can utilize the legs and the arms and provide full body motion. The position leg(s) can aid in the assembly task by adjusting the payload bay, reducing forces transferred to the truss. This is one of the large benefits of having positioning legs rather than using the arms for crawling and assembly.

Once the robot has completed the assembly, it returns back to the original starting location. This requires the system

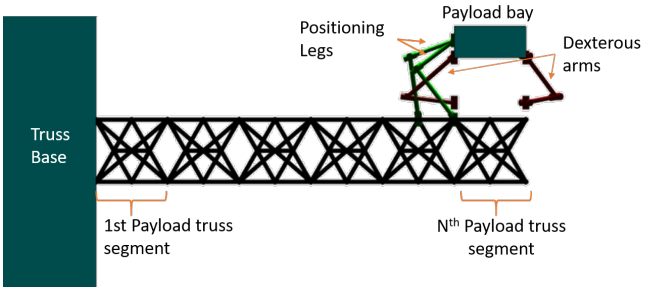

Fig. 2. Crawling Robot System

to crawl back along the truss; during this movement the dexterous arms remain still. Thus both the stationary and crawling systems start and end at the same point.

III. Sizing the System

A. Payload Truss Structure

While an ISA robot may be used for repairs, servicing, and inspection, the main task is assembly. Rather than focus on assembling individual trusses from beams, this study focuses on assembling completed truss segments together. This reduces the number of assembly steps that must be made and verified. Doggett et al. describes a Tri-Truss system, a structure which can collapse for packing and then be easily deployed [6]. One of the benefits is that these segments can have the science payloads, such as a telescope's mirror segments, mounted prior to launch. In addition, a large number of these segments can fit into one payload bay without greatly increasing the size. The two dexterous arms release the truss segment from the payload bay, deploy it to its final size, and lower it down into a desired position.

Many researchers are proposing the 10-25m range for the next large in-space telescope [2], [17], [15]. Here, the 20m truss is made up of a number of equal length segments which have attachment mechanisms allowing them to mount to each other. This case study focuses on building a 20m long rectangular truss structure.

Stiffness is an important factor when constructing long truss structures. The height and width of the final truss is based on a required minimal stiffness. The frequency for the completed structure can be found in equation 1. The material is assumed to be uniform throughout the structure with a Young's modulus of E. $I_{structure}$ is the moment of inertia for the completed structure. $L_{structure}$ is the total length of the constructed structure; in this study $L_{structure}$ is 20m. $M_{structure}$ is the mass of the structure and α is a coefficient based on the boundary conditions.

$$\omega = \frac{\alpha}{2\pi}\sqrt{\frac{EI_{structure}}{M_{structure}L^3_{structure}}} \tag{1}$$

Mikulas et al. [14] has established a method for estimating the diameter of a long truss based on the number of longerons and the desired stiffness. Figure 3 shows how this diameter relates to the actual shape of the truss. In this example, a

rectangular truss is used. The moment of Inertia can then be found using equation 2.

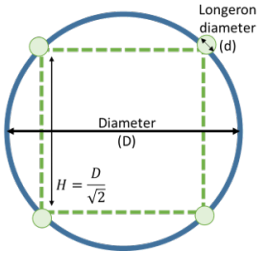

Fig. 3. Estimating the moment of Inertia for Truss

$$I_{structure} = \frac{D^2}{8} A_{longeron} N_{longeron} \tag{2}$$

$A_{longeron}$ and $N_{longeron}$ are the area and number of longeron, respectively. Using equations 1 and 2, along with the assumption that all the longerons have the same constant circular cross-section, then the diameter, D, of the truss segment can be calculated. Using this diameter, the height and width of the completed truss can be easily calculated.

During assembly, the truss must be able to withstand the force of a payload segment at its maximum acceleration. The inner and outer diameter of each longeron is calculated by treating the completed structure as a cantilever beam that must not buckle when subjected to a maximal force. This maximal force is generated by the dexterous arms moving a payload segment at their maximum arm acceleration. Operationally, the dexterous manipulators will not be operating at their maximum acceleration when carrying a truss segment near the rest of the structure. This simplification was made to ensure the structure would not buckle under worse-case conditions of the dexterous manipulators hitting the assembled truss with the piece they are assembling. For the crawling system, the positioning legs apply additional forces along the truss when they move themselves at the payload bay. The payload longerons are sized to ensure it will survive the assembly process either from the dexterous arms or the positioning legs.

B. Payload Bay Structure

The payload bay is assumed to be a simple structure used to house the payload segments before they are deployed and assembled. For a large number of truss segments (>20) this can lead to a tall payload bay. Mounting points for the dexterous arms and positioning legs are relative to the bottom of the payload bay, therefore, an increase in height does not change the total length of the manipulators. The dexterous arms are not sized to reach all the way into this enclosed environment. It is assumed that there is an internal mechanism used to ensure the next un-deployed truss segment is always at the bottom of the payload bay ready for the dexterous arms.

C. Manipulator Sizing Estimation

Each of the dexterous arms and the positioning leg(s) are 3DOF planar revolute manipulators. This will allow each manipulator to have full range of motion in this planar simulation. Each manipulator has two main links and a small tool tip. The third link, which is significantly smaller to allow for finer motions, allows the tool tip angle to be specified as part of the assembly task definition. As the pairs of manipulators work together, e.g. moving the payload bay or a payload segment into place, it is assumed the force is divided evenly among the paired manipulators. Evenly dividing the forces and moments is effective here because of to the symmetrical nature of this example and the trajectories chosen.

1) Total Length: Each of the robot systems use the same dexterous arms for handling of the individual truss segments. The total length of the dexterous manipulators are based primarily on the distance between the payload bay and the truss, which is set at twice the truss height to ensure there is room to deploy and maneuver each truss segment. The truss height is calculated based on the required stiffness for the final structure and does not change based on the robot system or the number of segments.

The number and the length of each individual truss segment is inversely proportionally to maintain a final completed truss length of 20m. In both robotic systems, the positioning leg(s) center the payload bay over the final position for the soon to be placed truss segment. Equation 3 shows that the total lengths of the positioning leg(s) depend on the type of robot, the truss segment length, P_{length}, the number of truss segments, N, and the payload height, P_{height}. C_{leg} is a sizing coefficient to ensure the positioning legs are not at the edge of their workspace. This value was calculated for each truss segment length to ensure the manipulator was able to reach the goal while still keeping the overall total length short. C_{leg} typically range from .9-1 for the stationary robot and 1.25-1.5 for the crawling system.

For a crawling robot, the positioning legs will become significantly shorter as the number of truss segments increases. However, for the stationary case the length of the positioning leg will increase as the number of segments increase. It should be noted that no packaging requirements were considered and no restrictions were placed on ensuring the individual link lengths were within any bounds of launch vehicles. As the manipulators lengths increase it may be necessary to add additional joints to ensure it fits within a launch vehicle.

$$\begin{aligned} L_{Leg_{stationary}} &= (P_{length}(N-1) + P_{Height}) C_{Leg} \\ L_{Leg_{crawling}} &= (P_{length} + P_{Height}) C_{Leg} \end{aligned} \tag{3}$$

2) Robot Dynamics: The joint angles, velocities, and accelerations are calculated for each of the manipulators based on the trajectories of the payload bay, truss segment, and the positioning leg mounting points. Using this information, the joint torques can then be calculated based on the force applied by each end-effector, see equation 4. Here, F is the

manipulator's dynamics expressed in Cartesian space where J is the Jacobian at specific joint angles θ, M_x is the mass matrix, V_x is the centrifugal and Coriolis terms, and G_x is the gravitational terms. The gravitational terms are zero due to the system only being designed to operate in space.

$$F = M_x(\theta)\ddot{X} + V_x(\theta,\dot{\theta}) + G_x(\theta) \tag{4}$$

The dexterous arms must produce the force required to move each payload truss segment through its desired trajectory; in this case, being lowered down from the payload bay and into place. This required force is evenly divided between the dexterous manipulators. During the dexterous arms' movement, the positioning leg(s) remain stationary and react the force to ensure the payload bay remains in place.

The force required to move the payload bay includes the mass of the dexterous manipulators and the remaining number of payload segments. During the dexterous arms' movements, the positioning leg(s) remain stationary in order to react the forces. In the case of the crawling system, when one leg is moving the other is stationary and reacts the forces to the payload truss. The design force for the positioning leg(s) depends on all of the these forces.

3) Robot Mass Estimation: In order to more accurately model the dynamics and the joint torques, the mass of each manipulator must be accounted for. The mass of the manipulators the summation of the estimated motor mass, the harmonic mass, and the structural mass.

The motor mass is found using the following mass estimation relations which uses the joint torque, T, and the joint speed, S in krpm, see equation 5. These equations are described in detail in [13]. They were found using heuristics taken from over 100 high-end DC brushless motors. The speed-torque curves for each motor was analyzed in order to determine the relationship between speed, torque, and mass. All masses are calculated in kilograms.

$$MotorMass = \begin{cases} 0.0676 + 1.3788T + 0.0010S & |T| < 3.17\text{Nm} \\ 2.5067 + 0.6071T - 0.2796S & |T| > 3.17\text{Nm} \end{cases} \tag{5}$$

Each motor is geared using harmonic gearing, which are often used in space robotics due to their compact size, light weight, and high gear ratio. This heuristic equation was found using data from multiple harmonic gears with ratios from 80:1 to 160:1. The mass of the harmonic gearing system is found in equation 6.

$$HarmonicMass = 0.0078T \tag{6}$$

The structural mass is calculated by treating the manipulator as if it were a stepped cantilever beam subject a force and a torque at the end. Each link is sized to minimize the robot mass while ensuring that all buckling, material, and maximum deflection constraints are met. Here, the buckling and the allowed maximum deflection drive the size of each link. See [13] for more detail on the manipulator mass estimation.

IV. Simulation Overview

A simulation, written in MatLAB using Peter Corke's Robotics Toolbox [5], is used to compare the two robotic systems. Figure 4 shows the major components of the simulation. The colored boxes indicate where an internal optimization function is used, for example optimizing the inner and outer diameter of each manipulator link while working to minimize the mass.

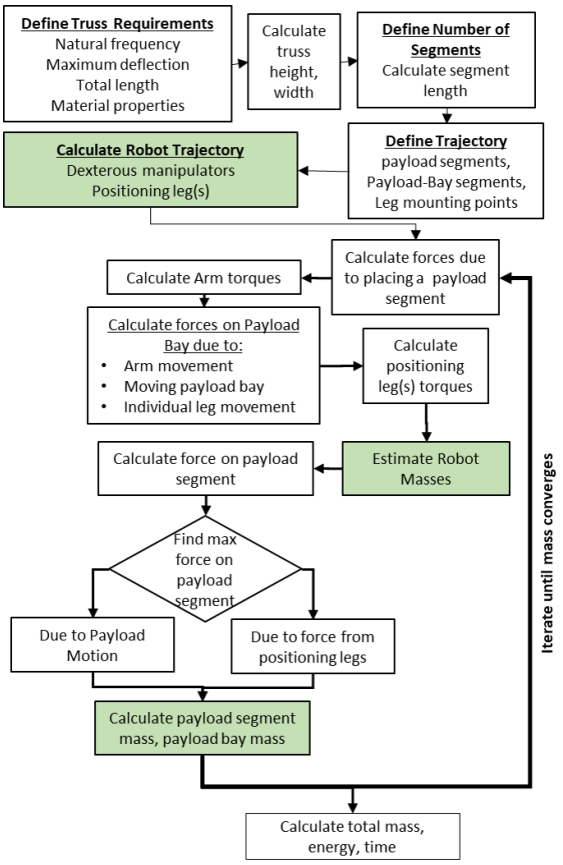

Fig. 4. Simulation Flow Diagram

Three metrics are used to compare the two robotic systems: the total mass of the systems, the time to complete the structure, and the required mechanical energy.

A. Mass Estimation

The total mass of the system includes the payload truss segments and the payload bay. It is assumed that the payload truss segments start in a non-deployed state so that all the segments can fit within the payload bay before being released. The payload bay length is assumed to be 10% bigger than that of a single payload segment, and the height is sized assuming each payload segment can collapse to 1/10 of its height.

B. Power Estimation

Power requirements can be a limiting factor for many space systems. The mechanical output power needed to move each robot is estimated, see equation 7. P is the mechanical

output power for a single joint, $\dot{q}$ is the joint velocity, and τ is the joint torque. Mechanical output power is not the only power needed, power for the computers and sensors is also required. It is assumed that the power required for these additional components is the same for both systems and are not included in this simulation.

$$P = \dot{q}\tau \tag{7}$$

C. Time Estimation

The total time is how long it takes to assemble the truss and then return to the original starting position. The maximum allowable accelerations for the payload bay and each payload segment are defined as the same for both the crawling and stationary systems. Under these assumptions, the crawling robot will always take more time because it must also move the positioning legs. Therefore, if time the complete the task is the driving requirement, then the stationary system is preferred.

V. Results

A. Externally Constrained Payload Segment

This first case looks at when an external constraint, such as launch loads or ground-based testing, is the driving design requirement for sizing the structural members of the payload truss segments. The outer and inner diameter of the truss segments are 0.25m and 0.2m, respectively, for all cases. Increasing the number of segments will reduce the individual segments length and mass, but the final assembled truss design will remain the same. There is a small 5% mass penalty for additional segments, in order to account for the connection points, joints, and mechanisms need to attach each segment to the main truss.

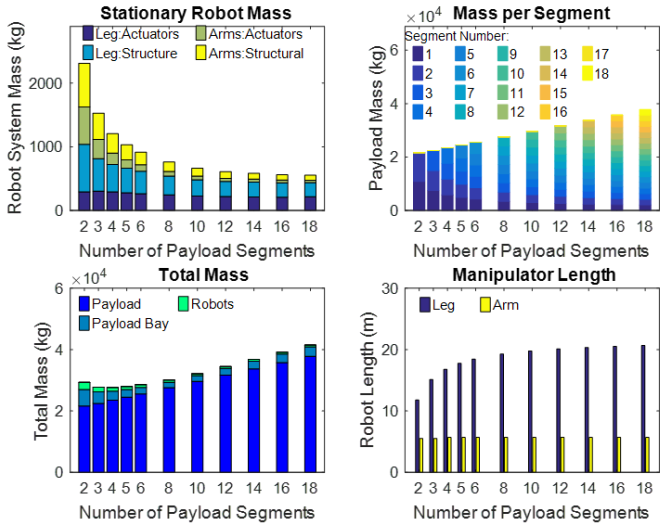

Fig. 5. Mass of stationary robotic system with payload structure sized by external loads and constraints

Figure 5 shows the results for a stationary robotic system as it constructs the final truss. Increasing the number of segments leads to a lighter weight stationary robot, however, there is a diminishing return as the number of segments increase.

The dexterous arms are sized to move individual payload segments and the trajectory for each payload remains the same regardless of the payload length. Decreasing the mass of each segment directly decreases the forces on the dexterous arms, reducing the actuator and structural mass.

The positioning leg moves the payload bay into place and, as the number of segments increases, it must increase in length in order to place the last segment. The mass being handled at the furthest point is reduced which reduces the load on the positioning leg. Increasing the length but reducing the design loads makes it difficult to conclude how changing the number of truss segments will affect the overall mass of the positioning leg. In this example, increasing the number of segments results in a small decrease in the positioning leg mass.

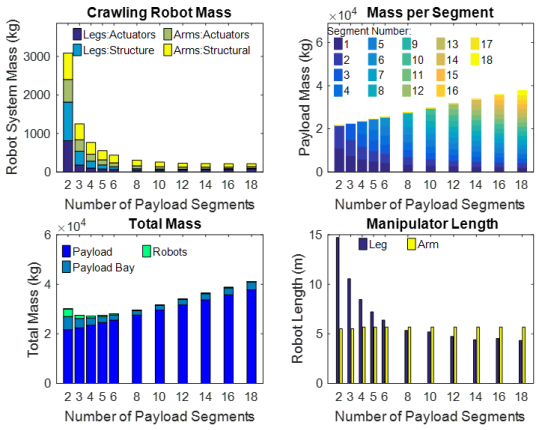

Fig. 6. Mass of crawling robotic system with payload structure sized by external loads and constraints

Figure 6 shows the results of the crawling robotic system assembling the same structure. The total payload mass increases exactly the same as in the previous case; thus the dexterous arms are the same for both the crawling and stationary robotic systems. The mass for the two positioning legs decrease as the number of segments increases. This is due to a reduction in leg length and in payload segment mass. This shorter length results in a much lower structural mass for each positioning leg.

Figure 7 compares the stationary and crawling robots as they assemble a truss with a predefined structural design. Both the stationary and crawling robot saw a decrease in mass as the number of segments increased. Though each robot system saw a large mass saving, the mass for the additional attachment mechanisms on the payload is more significant and, as a result, the entire system mass increases. This case emphasizes the need that the system be viewed as a whole and that focusing only on the robot does not necessarily result in a minimum mass system. The payload truss segments and the robot must be designed together.

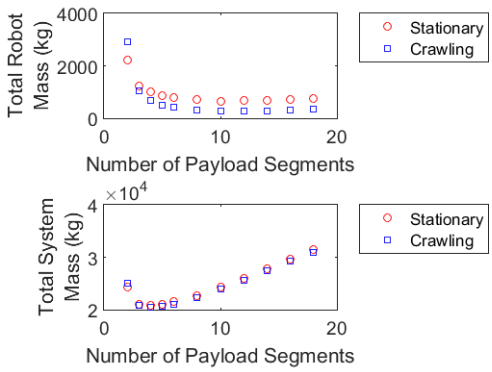

Fig. 7. Comparison between stationary and crawling systems for predefined payload structure

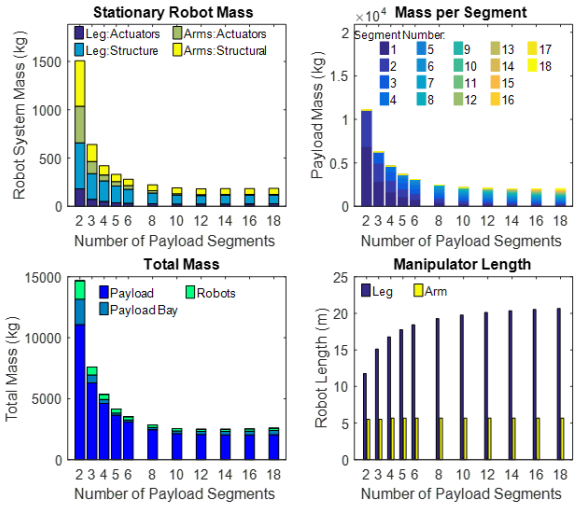

Fig. 8. Mass of stationary robot system with payload truss sizing determined by the assembly forces

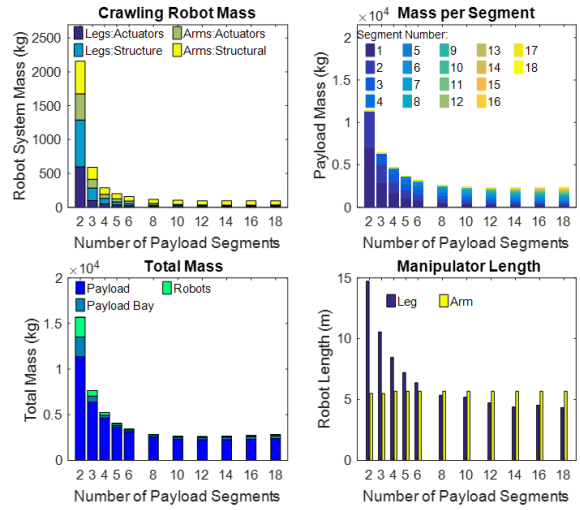

Fig. 9. Mass of crawling robot system with payload truss sizing determined by the assembly forces

B. Payload Segment Dictated by Assembly Loads

One of the benefits of ISA is that the final constructed structure does not have to be assembled on Earth and that, ideally, the design forces come from assembly and usage in space rather than from Earth-bound requirements. This next case looks at sizing the payload truss based on the in-space assembly forces rather than a previously chosen design point. The truss must be able to survive the assembly process: the maximum force/moment which occur as the last truss piece is added to the assembly. The payload truss is treated as a cantilever beam with forces and moments acting on the end, this is due to the maximum acceleration of the final payload segment.

Figure 8 shows the mass for the stationary robot and the truss payload when the truss is sized based on the in-space assembly forces. Figure 9 shows the results for the crawling robot when the assembly loads are the design forces for the payload truss. The payload truss here has the same mass as the stationary case because the truss is sized based on the same assembly forces.

Results show that stationary robot always has the greater mass of the two robotic systems except when the structure is only made of two pieces, see Figure 10. When the truss is made of only two segments, the stationary manipulator system is the more mass effective system. The crawling robot is sized to walk across each truss only grasping the corners. As such, for a two segment truss, the use of a crawling robot is not effective.

As the number of truss segments increase past two, the crawling robot always has a lower mass than the stationary robotic system. The two positioning legs in the crawling system are significantly smaller than the single positioning leg in the stationary system. However, mass is not the only metric that should be considered. Figure 11 shows that the time to complete the assembly is significantly higher for the crawling system, though the power required a less. As expected, the time to assembly the structure increases for both robotic systems as the number of segments increases.

C. Payload Segment Dictated by Large Crawling Forces

Assembly forces (forces on the truss resulting from assembling the last truss piece) are not always the driving design forces.

In addition to these forces, the truss in a crawling system must also be capable of reacting the forces from the positioning legs. These forces are from moving the payload bay and from holding the payload bay steady as the dexterous arms move individual pieces into place. Increasing the acceleration of the payload bay or the positioning legs will increase the forces the positioning legs will react to the truss. If not limited, these forces can easily exceed the previously used assembly forces thus, driving the design. The payload truss design for a crawling system and a stationary system are not guaranteed to be the same; a difference which may not be insignificant. As seen in previous results, the difference

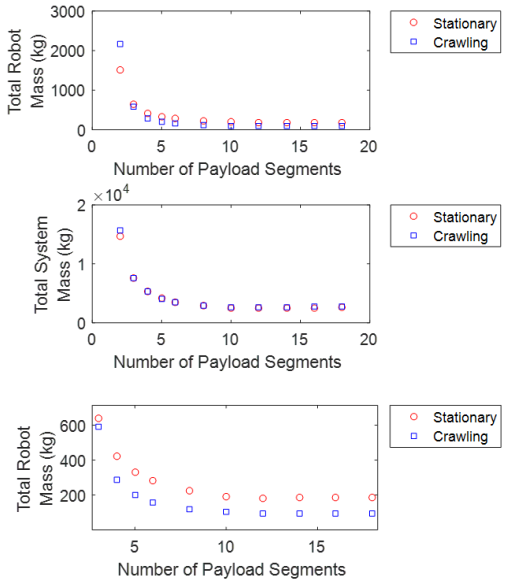

Fig. 10. Comparison between stationary and crawling systems when payload structure is sized based on the assembly force. Bottom graph is zoomed in to better show the robotic mass difference.

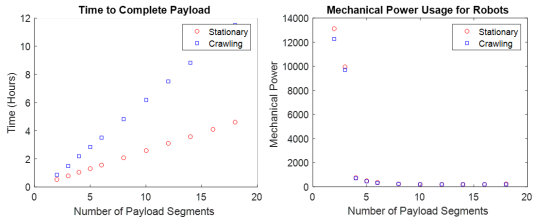

Fig. 11. Time (s) and mechanical power (Ws) when payload structure is sized based on the assembly force

between the stationary and crawling robots is on the order of 100kg and this difference is a very small fraction of the total system mass. A small increase in the mass of each payload segment can quickly result in the stationary system having the lower total mass, see Figure 12. As the number of truss segments increases, the crawling system has a lower robot mass though the stationary system has a lower system mass.

VI. Future Work

This study focuses on planar 3-DOF manipulators. Future work includes extending this study beyond the planar case to include full 6-DOF. As the simulation extends beyond the planar case, the symmetry between the manipulators is not guaranteed. The force distribution among the manipulators would need to be studied. Evenly dividing the forces works when the case is symmetric, as it was in this study, but relaxing that requirement would allow for more complex and optimized force distribution schemes.

The current simulation assumes the truss is being built from a unmoving truss base. This assumption holds for trusses being built off of very large bases, e.g. a solar panel truss on the ISS. For a stand-alone structure, like a space telescope, the truss base will not be significantly larger than

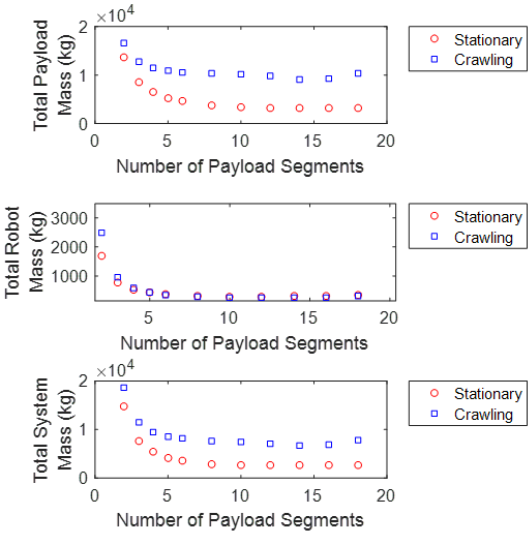

Fig. 12. Comparison between stationary and crawling systems when forces on the payload truss due to crawling exceed the assembly forces

the truss itself. In that case, the truss base itself needs to react the forces in-order to remain steady, which can be a requirement if the truss base contains the communication and power system.

Future ISA structures will have a large variety of lengths, based on science requirements. Here, a 20m long truss was shown in order to determine a method for comparing different robotic systems. Future work will include changing this total truss length to study how the total length of the truss also affects the assembly process and the robotic designs. Smaller truss systems, where the robot mass contributes significantly to the mass of the system, will be more driven by the robot design whereas larger systems, e.g. 100m diameter structure, will be driven by the structural design.

VII. Conclusion

This study compares crawling and stationary robotic systems as they assemble the same payload, a 20m long truss. The number of segments are varied and the systems are compared based on the mass, energy, and time it took to complete the truss. In all cases, the majority of the total system mass is from the payload truss mass. The robot mass represent only a small fraction of the total system mass.

Overall, the mass of each robot system decreases as the number of segments increases, though the delta mass savings decreases after a couple truss segments. As the number of segments increase, the individual segment mass decreases; resulting in a smaller mass for the dexterous arms and the positioning leg(s) to handle. In the case of the crawling robot, the length of the positioning legs greatly decreases, this further reduces the total robot mass.

The overall total system mass depends on the forces the robot applies to the payload truss. Forces from the robot crawling along truss can have a significant impact and can drive the payload mass. In such a case, though a crawling

robot may be less massive than a stationary system, the total system mass for the crawling system could be higher if care is not taken.

In-space assembly can be done by either a stationary robotic system or a crawling robotic system. The payload design and the robotic system both depend on each other and they should be designed together as a complete system rather than individual pieces.

REFERENCES

[1] JEREMY Banik. Realizing large structures in space. In *Proc., Frontiers of Engineering: Reports on Leading-Edge Engineering from the 2015 Symp*, pages 55–62, 2016.

[2] Wendel K Belvin, William R Doggett, Judith J Watson, John T Dorsey, Jay E Warren, Thomas C Jones, Erik E Komendera, Troy Mann, and Lynn M Bowman. In-space structural assembly: Applications and technology. In *3rd AIAA Spacecraft Structures Conference*, page 2163, 2016.

[3] Matthew R Bolcar, Steve Aloezos, Vincent T Bly, Christine Collins, Julie Crooke, Courtney D Dressing, Lou Fantano, Lee D Feinberg, Kevin France, Gene Gochar, et al. The large uv/optical/infrared surveyor (luvoir): Decadal mission concept design update. In *UV/Optical/IR Space Telescopes and Instruments: Innovative Technologies and Concepts VIII*, volume 10398, page 1039809. International Society for Optics and Photonics, 2017.

[4] William Bryan. Building in space: Government and industry meet to discuss in-space assembly, 2018.

[5] Peter I Corke. A robotics toolbox for matlab. *IEEE Robotics & Automation Magazine*, 3(1):24–32, 1996.

[6] William R Doggett, John Dorsey, John Teter, David Paddock, Thomas Jones, Erik E Komendera, Lynn Bowman, Chuck Taylor, and Martin Mikulas. Persistent assets in zero-g and on planetary surfaces: Enabled by modular technology and robotic operations. In *2018 AIAA SPACE and Astronautics Forum and Exposition*, page 5305, 2018.

[7] John Dorsey, William Doggett, Robert Hafley, Erik Komendera, Nikolaus Correll, and Bruce King. An efficient and versatile means for assembling and manufacturing systems in space. In *AIAA SPACE 2012 Conference & Exposition*, page 5115, 2012.

[8] Lee D Feinberg, Jason G Budinoff, Howard A MacEwen, Gary W Matthews, and Marc Postman. Modular assembled space telescope. *Optical Engineering*, 52(9):091802, 2013.

[9] Angel Flores-Abad, Ou Ma, Khanh Pham, and Steve Ulrich. A review of space robotics technologies for on-orbit servicing. *Progress in Aerospace Sciences*, 68:1–26, 2014.

[10] Mark Garcia. About the kibo laboratory, Jul 2017.

[11] Zainan Jiang, Zhiqi Li, Chongyang Li, Dapeng Yang, and Hong Liu. Design and preliminary ground experiment for robotic assembly of a modular space telescope. *IEEE Access*, 7:160870–160878, 2019.

[12] Nicolas N Lee, Joel W Burdick, Paul Backes, Sergio Pellegrino, Kristina Hogstrom, Christine Fuller, Brett Kennedy, Junggon Kim, Rudranarayan Mukherjee, Carl Seubert, et al. Architecture for in-space robotic assembly of a modular space telescope. *Journal of Astronomical Telescopes, Instruments, and Systems*, 2(4):041207, 2016.

[13] Katherine Marie McBryan. *TASK-BASED OPTIMIZATION OF MULTI-ARM SPACE ROBOTICS*. PhD thesis, 2018.

[14] Martin M Mikulas, Timothy J Collins, William Doggett, John Dorsey, and Judith Watson. Truss performance and packaging metrics. In *AIP Conference Proceedings*, volume 813, pages 1000–1009. AIP, 2006.

[15] Rudranarayan Mukherjeea. The future of space astronomy will be built: Results from the in-space astronomical telescope (isat) assembly design study rudranarayan mukherjeea*, nicholas sieglerb, & harley thronsonc. 2019.

[16] Angadh Nanjangud, Peter C Blacker, Alex Young, Chakravarthini M Saaj, Craig I Underwood, Steve Eckersley, Martin Sweeting, and Paolo Bianco. Robotic architectures for the on-orbit assembly of large space telescopes. In *Proceedings of the Advanced Space Technologies in Robotics and Automation (ASTRA 2019) symposium*. European Space Agency (ESA), 2019.

[17] Angadh Nanjangud, Craig I Underwood, Christopher P Bridges, Chakravarthini M Saaj, Steve Eckersley, Martin Sweeting, and Paolo Biancod. Towards robotic on-orbit assembly of large space telescopes: Mission architectures, concepts, and analyses. In *Proceedings of the International Astronautical Congress, IAC*, pages 1–25. International Astronautical Federation, 2019.

[18] John Nella, Paul D Atcheson, Charles B Atkinson, Doug Au, Allen J Bronowicki, Ed Bujanda, Andy Cohen, Don Davies, Paul A Lightsey, Richard Lynch, et al. James webb space telescope (jwst) observatory architecture and performance. In *Optical, Infrared, and Millimeter Space Telescopes*, volume 5487, pages 576–587. International Society for Optics and Photonics, 2004.

[19] Máximo A Roa, Korbinian Nottensteiner, Armin Wedler, and Gerhard Grunwald. Robotic technologies for in-space assembly operations. In *Proc. 14th Symp. Adv. Space Technol. Robot. Autom.*, 2017.

[20] Peter J Staritz, Sarjoun Skaff, Chris Urmson, and William Whittaker. Skyworker: a robot for assembly, inspection and maintenance of large scale orbital facilities. In *Proceedings 2001 ICRA. IEEE International Conference on Robotics and Automation (Cat. No. 01CH37164)*, volume 4, pages 4180–4185. IEEE, 2001.

[21] Harshit Suri, Peter Will, and Wei-Min Shen. System design of robots for application to in-space assembly. In *2006 IEEE/RSJ International Conference on Intelligent Robots and Systems*, pages 5100–5105. IEEE, 2006.